

## Accepted Article

**Title:** Self-stabilized Amorphous Organic Room Temperature Phosphorescence

**Authors:** Wei Xu, Yaguo Yu, Xiaonan Ji, Huarui Zhao, Jinming Chen, Yanyan Fu, Huimin Cao, Qingguo He, and Jiangong Cheng

This manuscript has been accepted after peer review and appears as an Accepted Article online prior to editing, proofing, and formal publication of the final Version of Record (VoR). This work is currently citable by using the Digital Object Identifier (DOI) given below. The VoR will be published online in Early View as soon as possible and may be different to this Accepted Article as a result of editing. Readers should obtain the VoR from the journal website shown below when it is published to ensure accuracy of information. The authors are responsible for the content of this Accepted Article.

**To be cited as:** *Angew. Chem. Int. Ed.* 10.1002/anie.201906881  
*Angew. Chem.* 10.1002/ange.201906881

**Link to VoR:** <http://dx.doi.org/10.1002/anie.201906881>  
<http://dx.doi.org/10.1002/ange.201906881>

# Self-stabilized Amorphous Organic Room Temperature Phosphorescence

Wei Xu<sup>[a]</sup> [b], Yaguo Yu<sup>[a]</sup> [b], Xiaonan Ji<sup>[a]</sup> [b], Huarui Zhao<sup>[a]</sup>, Jinming Chen<sup>[a]</sup> [b], Yanyan Fu<sup>[a]</sup> [b], Huimin Cao<sup>[a]</sup>, Qingguo He<sup>[a]</sup> [b] and Jiangong Cheng<sup>[a]</sup> [b]

**ABSTRACT:** The stability of pure organic room-temperature phosphorescent (RTP) materials in air is one of the research hotspot in recent years. Without crystallization or encapsulation, a new strategy was proposed to obtain self-stabilized organic RTP materials, based on a complete ionization of photo-induced charge separation system. The ionization of aromatic phenol 4-carbazolyl salicylaldehyde (CSA), formed a stable H-bonding anion-cation radical structure, and led to the completely amorphous CSA-I film. Long phosphorescent lifetime was gained as long as 0.14 s at room temperature and a direct exposure in air. The emission intensity was also increased by 21.5 times. Such amorphous RTP material reconciled the contradiction between phosphorescence stability and vapor permeability, and has been successfully utilized for peroxide vapor detection.

Recently, pure organic room-temperature phosphorescence (RTP) with long afterglow has become a research hotspot for its potential applications in wide areas such as biological imaging, digital encryption, opto-electronic devices.<sup>[1, 2]</sup> Meanwhile, because of the long excited-state relaxation lifetime, phosphorescent materials also show great value in catalysis, sensing, and photovoltaic fields.<sup>[3]</sup>

Much progress has been achieved in long lifetime RTP materials, based on different kinds of molecule structures, from carbazole derivatives<sup>[4, 5]</sup>, diphenyl ketone derivatives<sup>[6-8]</sup>, phenothiazine derivatives,<sup>[9, 10]</sup> imide compounds<sup>[11]</sup>, aromatic carboxylic acid derivatives<sup>[12]</sup> to AIE luminogens<sup>[13]</sup>. Among these materials, the RTP efficiency can be as high as 34.5% via 1-(dibenzo[b,d]furan-2-yl)phenylmethanone structure, while the RTP lifetime can be as long as 1360 ms via isophthalic acid structure. However, phosphorescent materials still suffered a vital problem-- stability. The triplet excited states of RTP materials are so unstable that they can be quenched under many circumstances, from triplet state molecules like oxygen, to non-radiative molecular vibration at room temperature.

To avoid these adverse factors, most RTP molecules have been prepared as crystalline structure<sup>[14-16]</sup>, with restricted molecule motion and low air permeability.<sup>[17]</sup> Other strategies were also adopted such as encapsulation in polymer package<sup>[18, 19]</sup> or formation of host-guest complexes to eliminate the

influence of O<sub>2</sub><sup>[20]</sup>. Whether in crystalline and tight packaging state, non-radiative vibration deactivation or contact with the triplet quenching agents could be suppressed, leading to a higher phosphorescence efficiency. However, the permeability of its film would be sacrificed together with them, which limited its potential applications in the fields of catalysis and sensing.

In 2017, Adachi group reported an ultra-long persistent luminescent material based on organic photo-induced charge separation system.<sup>[21]</sup> Via low energy density laser excitation, the neutral host-guest molecule pair of strong electron-accepting molecule 2,8-bis(diphenylphosphoryl)dibenzo[b,d] thiophene (PPT) and strong electron-donating molecule N,N,N',N'-tetramethylbenzidine (TMB) can be effectively converted into radical ion pairs, lengthening the phosphorescence lifetime to minute level.<sup>[22]</sup> However, although the structure was in amorphous state, the luminescent components still need the protection of tight polymer encapsulation against air.

Constructing ionic structure with multiple hydrogen bonds is another effective method for lengthening RTP lifetime, reported as RTP organic ionic crystals.<sup>[23-25]</sup> Inspired by the photo-induced charge separation and ionic crystals, we considered about constructing a completely ionized system to gain ultra-stable amorphous phosphorescent system. As Figure 1a and 1b shows, instead of crystalline protection or polymer encapsulation, the electrostatic interaction among ion pairs, together with other inter-molecular interaction, for example, hydrogen bonding interaction,<sup>[26]</sup> can probably enhance the occurrence of triplet excited state and gain more stable long lifetime RTP in air.

To obtain such a completely ionized system, aromatic aldehyde molecules were chosen as the basic structure for its potential phosphorescent capacity. Phenol group was introduced into aromatic aldehyde molecules to form a salicylaldehyde structure for the ionization upon a simple reaction between amine and the phenol group. So an anion-cation pair was obtained with the electron donating phenol anion and the electron accepting amine cation. Due to the existence of both oxygen and nitrogen and hydrogen atoms, hydrogen bonding interaction may also be formed between the anion-cation pairs. With this design, it is expected to realize an air stable room phosphorescence emission despite its amorphous morphology.

Based on the discussion above, CSA-I with a carbazole backbone was designed as the target compound. The salicylaldehyde CSA and carbazolyl *p*-benzaldehyde CBA were used for comparison to understand the effect of the ionization and the phenol unit on the phosphorescent property. The synthetic routes of the above-mentioned compounds were given in Scheme 1. CBA and CSA were synthesized under microwave condition. CSA-I was synthesized by a reaction of CSA and diethylamine (DEA) at room temperature.

[a] Dr. Wei Xu, Yaguo Yu, Xiaonan Ji, Huarui Zhao, Jinming Chen, Dr. Yanyan Fu, Huimin Cao, Prof. Qingguo He, Prof. Jiangong Cheng  
State Key Lab of Transducer Technology, Shanghai Institute of Microsystem and Information Technology, Chinese Academy of Sciences, Changning Road 865, Shanghai 200050, China.

E-mail: [windxu@mail.sim.ac.cn](mailto:windxu@mail.sim.ac.cn); [hqg@mail.sim.ac.cn](mailto:hqg@mail.sim.ac.cn); [jgcheng@mail.sim.ac.cn](mailto:jgcheng@mail.sim.ac.cn);  
Fax: +86-21-62511070-8934; Tel: +86-21-62511070-8967.

[b] Dr. Wei Xu, Yaguo Yu, Xiaonan Ji, Jinming Chen, Dr. Yanyan Fu, Prof. Qingguo He, Prof. Jiangong Cheng

Center of Materials Science and Optoelectronics Engineering, University of the Chinese Academy of Sciences, Yuquan Road 19, Beijing, 100039, China

Supporting information for this article is given via a link at the end of the document.

## COMMUNICATION

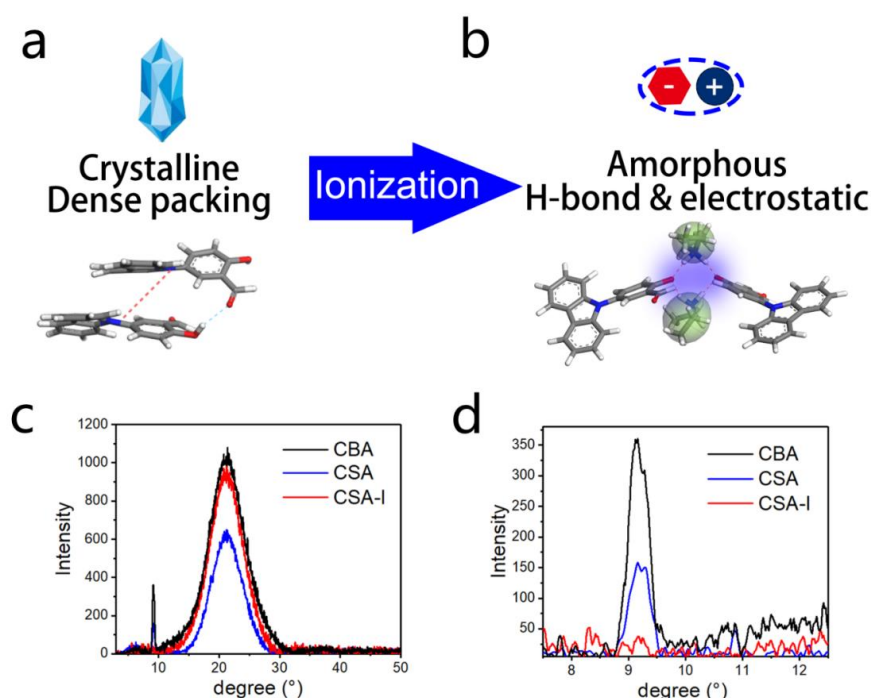


**Figure 1** (a),(b)The sketch diagram of the transformation from crystalline CSA structure to the ionized CSA-I structure. (c),(d) XRD spectra of CBA (black),CSA (blue) and CSA-I (red) films.

To evaluate the effect of the ionization of CSA by DEA, the morphology of the films was characterized by X-ray diffraction (XRD) and scanning electron microscopy (SEM). Both CBA and CSA film showed a diffraction peak near 9° diffraction angle and a broad diffuse scattering peak from 15° to 22°, while CSA-I film has no such a sharp peak but with only the diffuse scattering peak corresponding to an amorphous structure as indicated in Figure 1c and 1d. SEM images in Figure S1a–e indicate that CBA tends to form crystalline micro-rod structure (~1 μm), CSA is incline to show a crystalline nanoparticles (~100 nm) together with micro-rod structures (~1 μm), while CSA-I film is composed of amorphous nanoparticles (~100 nm), suggesting that the introduction of phenol and/or DEA will have a great influence on the morphology of their films.

Figure 2 showed the fluorescent and phosphorescent spectra of the three film samples. Under the UV excitation at 340 nm, the fluorescent peaks of CBA sample centred at 393, 416 and 443 nm, while the peaks of CSA and CSA-I samples were located around 430 nm and 450 nm, as shown in Figure 2a. The fluorescent lifetimes of CBA, CSA and CSA-I were 4.11, 2.56 and 1.99 ns, respectively. Different from their fluorescent spectra, Figure 2b indicates that the phosphorescent peaks centred at ~540 nm for CSA and CSA-I. The phosphorescent intensity of CSA-I film is 21.5 times stronger than that of CSA film, even 3 times stronger than that of CBA film (centred at 590 nm) under the same condition. Meanwhile, the phosphorescence quantum yield of CSA-I increased by 19.3 times relative to CSA (from 0.22% to 4.16%). The phosphorescent lifetime curves of CSA and CSA-I were measured with emission at 540 nm and excitation at 340 nm. According to the curve fitting data, the lifetime of CSA-I film was 0.14 s, much longer than that of CSA film (30 ms). Evidently, the ionization of CSA could greatly increase both the phosphorescent intensity and the phosphorescent lifetime.

As mentioned above, amorphous film will be much better in vapor permeability than that of crystal or encapsulated film. Associated with our previous work about peroxide probe<sup>[27]</sup>, we demonstrated the phosphorescent sensing properties of CSA-I to H<sub>2</sub>O<sub>2</sub> vapor. As shown in Figure 2c, after reacting with saturated H<sub>2</sub>O<sub>2</sub> vapor for 30 s, the lifetime of CSA-I film rapidly declined from 0.14 s to 27 ms. Besides lifetime change, the relationship curves of both fluorescent and phosphorescent peak intensity with time of CSA-I film were also measured as shown in Figure 2d. The phosphorescence of CSA-I film was so stable that the emission intensity even increased by 2.8% in air condition at room temperature. When it is exposed to H<sub>2</sub>O<sub>2</sub> vapor, the phosphorescence was quenched by 30% in 300 s. As comparison, the fluorescence of CSA-I film was bleached by 24.3% in air and quenched by 41.1% in H<sub>2</sub>O<sub>2</sub> vapor.

Both the FL and PL quenching processes were caused by the oxidation of aldehyde group to carboxylic acid unit (reaction schematic shown in Scheme 1), which is reactive in its ionization state.<sup>[27]</sup> The active carboxylic acid made the phenol anion protonated to form neutral phenol, therefore, the charge separation system was destroyed and the RTP emission was quenched efficiently. The RTP effect of CSA-I film and its phosphorescence sensing process in H<sub>2</sub>O<sub>2</sub> vapor were directly captured by camera as shown in Figure 2e. From 0 ms to 40 ms, the emission intensity gradually decreased, which shows the intensity of oxidized CSA-I (right) remains the weaker emission level compared with the sample without reaction (left). The photo induced charge separation process continuously enhances the emission intensity at phosphorescent mode, meanwhile, decrease the emission intensity at fluorescent mode. Therefore, the phosphorescent mode of CSA-I amorphous film can better avoid photo-bleaching effect and reduce noise signal, leading to a better sensing performance than fluorescent mode.



## COMMUNICATION

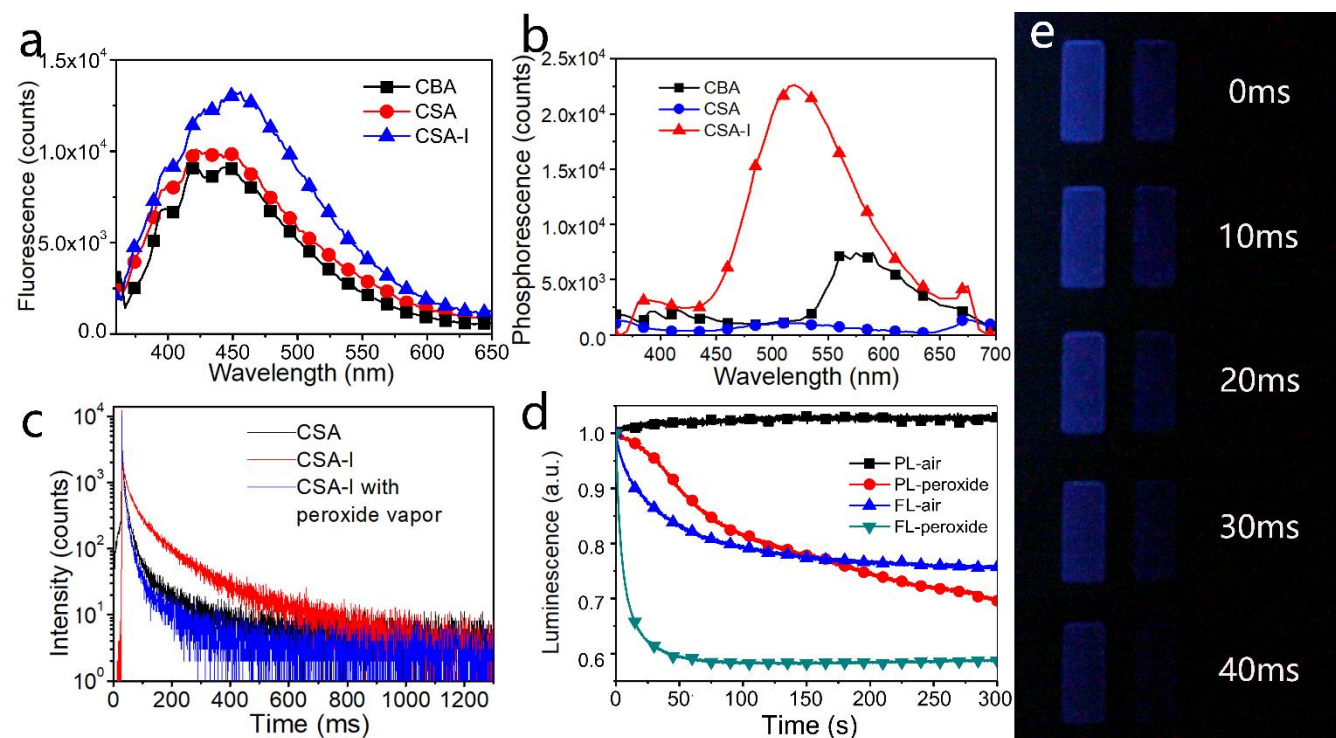


**Figure 2** The film state (a) fluorescent spectra and (b) phosphorescent spectra of CBA (black), CSA (red) and CSA-I (blue). (c) Lifetime curves of CSA (black), CSA-I (red) and CSA-I reacted with saturated  $\text{H}_2\text{O}_2$  vapor, excitation at 340nm, emission at 540 nm. (d) Phosphorescence time curves in air (black) and in  $\text{H}_2\text{O}_2$  vapor (red) and fluorescent time curves in air (blue) and in saturated  $\text{H}_2\text{O}_2$  vapor (green). (e) Photographs of film state CSA-I before (left) and after (right) reacting with saturated  $\text{H}_2\text{O}_2$  vapor, at 0ms, 10ms, 20ms, 30 ms, 40ms, 50ms and 60 ms after switching off 254 nm UV lamp, captured by camera SONY  $\alpha 6300$  at 1/100 s shutter speed.

Different with the crystal and encapsulated phosphorescence material, the reason for the such a stable amorphous RTP material CSA-I should be uncovered. The mechanism was systematically analysed by both theoretical simulations and transient absorption spectra characterizations.

The self-assembling behaviours of CSA-I, CBA, and CSA molecules were simulated by putting their four respective molecules into an isothermal-isobaric system (Figure 3a). After a 50 ps dynamic process, each two CSA-I ion pairs tend to form a stable dimer structure, connected by quadruple hydrogen bonds. With the formation of dimer structure, the potential energy decreased by 79.2% (from 87.23 to 18.10 kcal/mol). Meanwhile, the density of CSA-I system also greatly increased by 61.8% (from 0.089 to 0.144 g/cm<sup>3</sup>). After the same dynamic process, CBA and CSA molecules demonstrated ordered arrangement (Figure S2), but the potential energy change of CSA was just 8.6%, far lower than that of CSA-I. Movies of the dynamic simulation processes are available in SI (avi format movies). Therefore, in spite of lack crystal lattice or package polymer for a stable structure, the formation of stable dimers in the CSA-I film could act the same role. As a result, the non-radiative relaxation was suppressed by electrostatic and hydrogen bonding interactions without sacrificing its permeability in the amorphous film of CSA-I.

Figure 3b indicated that both the ground state (blue) and triplet state  $T_1$  orbital (red) of CSA-I dimer delocalized on the two different aromatic units as  $\pi$  orbitals, hence the transition was long-lifetime  $^3(\pi, \pi^*)$  type. In contrast, as Figure 3c shows, the  $T_1$  orbital of CSA-I monomer mainly localized on the  $\text{Et}_2\text{NH}_2^+$  cation, while its  $S_1$  orbital localized near the formaldehyde group, indicating a short-lifetime  $^3(n, \pi^*)$  transition for  $T_1 \rightarrow S_0$  and a  $^1(n, \pi^*)$  type transition for  $S_1 \rightarrow S_0$ . Since inter-system transition between the same orbital type is inhibited, and the existence time of  $(\pi, \pi^*)$  type  $T_1$  state in dimer structure is longer, thus the formation of ionized dimer structure is advantageous for increasing both the phosphorescence efficiency and prolonging the lifetime of the RTP material.

Furthermore, Ma *et al.* reported that the strong electrostatic interaction can further enhance the radiative decay and hinder the non-radiative decay of phosphorescent materials [28]. For the dimer structure in CSA-I system, both the strong electrostatic interaction of ionic bonds and the strong interaction of the quadruple hydrogen bonds, mainly distributed between the two phenol anions. Such highly centralized strong interactions can obviously enhance the triplet radiative transition process. Here the anion- $\pi$  interactions of the ionized system also enhance the inter-system crossing process, act like external heavy atom effect. [29]

## COMMUNICATION

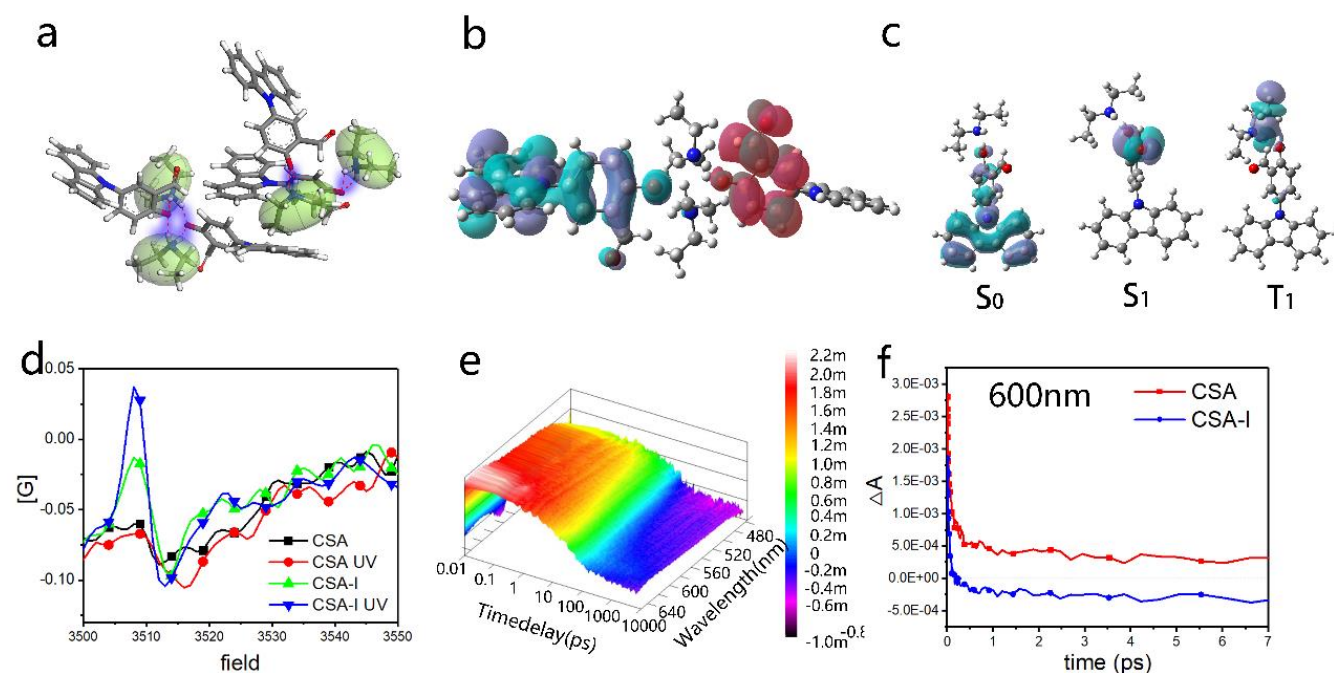


**Figure 3** (a) Space distribution of CSA-I before and after 50 ps isothermal-isobaric dynamics simulation, simulated with the Forcite plus module in Materials Studio 8. (H-bonds highlighted as shining dot-lines) (b) Ground state  $S_0$  (blue) and triplet excited state  $T_1$  (red) orbital distributions of CSA-I H-bonding dimer structure. (c) Ground state  $S_0$ ,  $S_1$  and triplet excited state  $T_1$  orbital distributions of CSA-I monomer. (d) Electron paramagnetic resonance spectra of CSA (black), CSA-I (green), CSA under UV light (red) and CSA-I under UV light (blue). (e) 3D broadband transient absorption spectra of CSA-I film. (f) Transient absorption spectra kinetics curves of CSA (red) and CSA-I (blue) film.

Electron para-magnetic resonance spectrum was used for CSA-I film characterization whatever before or after UV irradiation at a wavelength of 365 nm (Figure 3d). Compared with CSA film before UV excitation, an extra peak at 3508 Gs was observed, the intensity doubled under UV excitation. These phenomena suggest the film has a radical character before the UV excitation and enhanced radicals after UV irradiation. The comparison of the UV-vis absorption spectra of CSA and CSA-I (Figure S10) suggests that, the  $\pi$ - $\pi^*$  related absorption peak in CSA at 250 nm split into two peaks in CSA-I at 240 nm and 260 nm, probably caused by the formation of the radical specie. The increased radical character means that more ion pairs were transferred to the radiation cycle, which is supported by the ground state bleaching signal (a continuous concentration loss of ground state exciton) via its kinetics curves of transient absorption spectrum. Figure 3f demonstrated, during a 7 ps kinetic process, the intensity of CSA-I rapidly decreased to negative value in 300 fs, while the intensity of CSA just gradually approached the zero line.

As reported, the formation of extra radical pair is beneficial for enhancing the spin-orbit coupling and the intersystem crossing process from singlet state to triplet state<sup>[30]</sup>, which also contribute to the increased phosphorescent performance.

Such designing strategy of ultra-stable amorphous RTP system is also applicable to other aromatic molecules. For example, through the introduction of phenol group on 2,4,6-triformyl benzene and naphthaldehyde, two materials without phosphorescent property were gained: 2,4,6-triformyl-phenol (TFP) and formyl-naphthol (DFN). After the same ionization

process as CSA-I, the lifetime of the amorphous TFP-I and DFN-I were 0.33 ms and 55  $\mu$ s, respectively, far longer than their neutral state lifetimes of 0.4 ns and 2 ns.

In conclusion, we have developed a new strategy to obtain ultra-stable organic RTP materials without crystallization or encapsulation, based on completely ionized photo-induced charge separation system. Two RTP materials, CSA-I and TFP-I has been obtained, with lifetimes as long as 0.16 s and 0.33 ms, respectively. Both the stability and permeability of these amorphous RTP materials are so good that they have even been successfully applied in detection of peroxide vapor. This work may bring new designing strategy of pure organic RTP materials, and expand their application area to many new fields such as catalysis and vapor detection.

## Acknowledgment

This work is supported by the research Programs from Ministry of Science and Technology (Grant No.: 2016YFA0200800), the National Natural Science Foundation of China (Grant Nos. 61831021, 61771460 and 51641307), and Shanghai Sailing Program (No. 19YF1455700). We would also like to express thanks to Prof. Jinqian Chen and Dr. Xiaoxiao He (East China Normal University) for their assistance about transient absorption spectra.

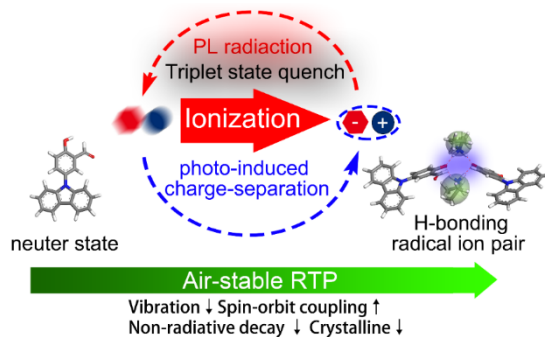
## References

## References:

- [1] Y. Liu, G. Zhan, Z. Liu, Z. Bian, C. Huang, *Chinese Chem. Lett.* **2016**, 27, 1231.
- [2] Y. Xie, Y. Ge, Q. Peng, C. Li, Q. Li, Z. Li, *Adv. Mater.* **2017**, 29, 1606829.
- [3] S. Richert, G. Bullard, J. Rawson, P. J. Angiolillo, M. J. Therien, C. R. Timmel, *J. Am. Chem. Soc.* **2017**, 139, 5301.
- [4] Z. An, C. Zheng, Y. Tao, R. Chen, H. Shi, T. Chen, Z. Wang, H. Li, R. Deng, X. Liu, W. Huang, *Nat. Mater.* **2015**, 14, 685.
- [5] S. Cai, H. Shi, Z. Zhang, X. Wang, H. Ma, N. Gan, Q. Wu, Z. Cheng, K. Ling, M. Gu, C. Ma, L. Gu, Z. An, W. Huang, *Angew. Chem. Int. Edit.* **2018**, 57, 4005.
- [6] W. Zhao, Z. He, J. W. Y. Lam, Q. Peng, H. Ma, Z. Shuai, G. Bai, J. Hao, B. Z. Tang, *Chem* **2016**, 1, 592.
- [7] Z. He, W. Zhao, J. W. Y. Lam, Q. Peng, H. Ma, G. Liang, Z. Shuai, B. Z. Tang, *Nat. Commun.* **2017**, 8, 416.
- [8] C. Li, X. Tang, L. Zhang, C. Li, Z. Liu, Z. Bo, Y. Q. Dong, Y. Tian, Y. Dong, B. Z. Tang, *Adv. Opt. Mater.* **2015**, 3, 1184.
- [9] J. Yang, X. Zhen, B. Wang, X. Gao, Z. Ren, J. Wang, Y. Xie, J. Li, Q. Peng, K. Pu, Z. Li, *Nat. Commun.* **2018**, 9, 840.
- [10] S. Tian, H. Ma, X. Wang, A. Lv, H. Shi, Y. Geng, J. Li, F. Liang, Z. Su, Z. An, W. Huang, *Angew. Chem. Int. Edit.* **2019**, 58, 6645.
- [11] X. Chen, C. Xu, T. Wang, C. Zhou, J. Du, Z. Wang, H. Xu, T. Xie, G. Bi, J. Jiang, X. Zhang, J. N. Demas, C. O. Trindle, Y. Luo, G. Zhang, *Angew. Chem. Int. Edit.* **2016**, 128, 10026.
- [12] Y. Gong, L. Zhao, Q. Peng, D. Fan, W. Z. Yuan, Y. Zhang, B. Z. Tang, *Chem. Sci.* **2015**, 6, 4438.
- [13] W. Z. Yuan, X. Y. Shen, H. Zhao, J. W. Y. Lam, L. Tang, P. Lu, C. Wang, Y. Liu, Z. Wang, Q. Zheng, J. Z. Sun, Y. Ma, B. Z. Tang, *J. Phys. Chem. C* **2010**, 114, 6090.
- [14] Z. An, C. Zheng, Y. Tao, R. Chen, H. Shi, T. Chen, Z. Wang, H. Li, R. Deng, X. Liu, W. Huang, *Nat. Mater.* **2015**, 14, 685.
- [15] C. Tang, R. Bi, Y. Tao, F. Wang, X. Cao, S. Wang, T. Jiang, C. Zhong, H. Zhang, W. Huang, *Chem. Commun.* **2015**, 51, 1650.
- [16] Y. Gong, L. Zhao, Q. Peng, D. Fan, W. Z. Yuan, Y. Zhang, B. Z. Tang, *Chem. Sci.* **2015**, 6, 4438.
- [17] O. Bolton, K. Lee, H. Kim, K. Y. Lin, J. Kim, *Nat. Chem.* **2011**, 3, 205.
- [18] T. Ogoshi, H. Tsuchida, T. Kakuta, T. Yamagishi, A. Taama, T. Ono, M. Sugimoto, M. Mizuno, *Adv. Funct. Mater.* **2018**, 1707369.
- [19] S. Tao, S. Lu, Y. Geng, S. Zhu, S. A. T. Redfern, Y. Song, T. Feng, W. Xu, B. Yang, *Angew. Chem. Int. Edit.* **2018**, 57, 2393.
- [20] D. Li, F. Lu, J. Wang, W. Hu, X. Cao, X. Ma, H. Tian, *J. Am. Chem. Soc.* **2018**, 140, 1916.
- [21] R. Kabe, C. Adachi, *Nature* **2017**, 550, 384.
- [22] H. Ohkita, W. Sakai, A. Tsuchida, M. Yamamoto, *Macromolecules* **1997**, 30, 5376.
- [23] G. Chen, H. Feng, F. Feng, P. Xu, J. Xu, S. Pan, Z. Qian, *J. Phys. Chem. Lett.* **2018**, 9, 6305.
- [24] B. Zhou, D. Yan, *Adv. Funct. Mater.* **2019**, 29, 1807599.
- [25] W. Chen, Z. Tian, Y. Li, Y. Jiang, M. Liu, P. Duan, *Chem. Eur. J.* **2018**, 24, 17444.
- [26] L. Bian, H. Shi, X. Wang, K. Ling, H. Ma, M. Li, Z. Cheng, C. Ma, S. Cai, Q. Wu, N. Gan, X. Xu, Z. An, W. Huang, *J. Am. Chem. Soc.* **2018**, 140, 10734.
- [27] W. Xu, Y. Fu, Y. Gao, J. Yao, T. Fan, D. Zhu, Q. He, H. Cao, J. Cheng, *Chem. Commun.* **2015**, 51, 10868.
- [28] H. Ma, W. Shi, J. Ren, W. Li, Q. Peng, Z. Shuai, *J. Phys. Chem. Lett.* **2016**, 7, 2893.
- [29] J. Wang, X. Gu, H. Ma, Q. Peng, X. Huang, X. Zheng, S. H. P. Sung, G. Shan, J. W. Y. Lam, Z. Shuai, B. Z. Tang, *Nat. Commun.* **2018**, 9, 2963.
- [30] H. Tsubomura, R. S. Mulliken, *J. Am. Chem. Soc.* **1960**, 82, 5966.

## COMMUNICATION

Ultra-stable organic RTP without crystallization or encapsulation, based on new designing strategy of completely ionized photo-induced charge separation. The RTP lifetime was lengthened to 0.16 s while the intensity was increased by 21.5 times. The excellent permeability of amorphous RTP system expand their application to vapor detection.



Wei Xu\*, Yaguo Yu, Xiaonan Ji, Huarui Zhao, Jinming Chen, Yanyan Fu, Huimin Cao, Qingguo He\* and Jiangong Cheng\*

Page No. – Page No.

**Self-stabilized Amorphous Organic Room Temperature Phosphorescence**